AIP | Journal of Renewable and Sustainable Energy

LiFePO4 battery state of charge estimation based on the improved Thevenin equivalent circuit model and Kalman filtering

Zhu Xu, Shibin Gao, and Shunfeng Yang

Citation: Journal of Renewable and Sustainable Energy **8**, 024103 (2016); doi: 10.1063/1.4944335
View online: http://dx.doi.org/10.1063/1.4944335
View Table of Contents: http://scitation.aip.org/content/aip/journal/jrse/8/2?ver=pdfcov
Published by the AIP Publishing

$LiFePO_4$ battery state of charge estimation based on the improved Thevenin equivalent circuit model and Kalman filtering

Zhu Xu,[1,a)] Shibin Gao,[1] and Shunfeng Yang[2]
[1]*School of Electrical Engineering, Southwest Jiaotong University, Chengdu 610031, China*
[2]*School of Electrical and Electronic Engineering, Nanyang Technological University, Singapore 639798, Singapore*

(Received 23 June 2015; accepted 26 February 2016; published online 29 March 2016)

Lithium iron phosphate ($LiFePO_4$) batteries are widely used as power batteries for electric vehicle applications. For safety issues, it is important to estimate the State of Charge (SOC) of a battery accurately. The improved Thevenin equivalent circuit model is established according to the characteristics of the $LiFePO_4$ battery, and the model parameters are identified by experimental testing. Furthermore, a novel algorithm of SOC online estimation is proposed, which combines the open-circuit voltage method, ampere-hour integration, and Kalman filtering. The simulations and experimental results show that the improved Thevenin equivalent circuit model can enhance the accuracy of SOC estimation. This proposed algorithm could estimate the SOC precisely even with inaccurate initial values and current measurement errors and distinguish the performances between the batteries. The performance of the proposed SOC estimation method when the voltage sensor is unavailable has been investigated and presented as well. From the characteristics mentioned above, this novel approach is able to guarantee the reliability and safety of the batteries. © *2016 AIP Publishing LLC*. [http://dx.doi.org/10.1063/1.4944335]

I. INTRODUCTION

The automobile industry has been increasing the penetration of electric vehicles (EVs) in the market because of the annual reduction in global oil resources. Lithium iron phosphate ($LiFePO_4$) battery packs are widely used as power supplies for EV. In practice, the $LiFePO_4$ battery is usually configured in series or parallel in order to achieve a higher voltage level or larger capacity. The differences of dynamic characteristic among batteries would cause the State of Charge (SOC) to be unbalanced, as well as inevitably influence the efficiency and lifetime of the battery packs. Therefore, it is significant to estimate the SOC of the $LiFePO_4$ battery in real-time in order to ultimately improve the battery performance and lengthen the useful lifetime of battery packs.

SOC must be estimated by some algorithm since it is not a direct measurement. Estimating the SOC of a $LiFePO_4$ battery accurately, based on measurement of battery physical quantities (e.g., battery voltage and current), is a challenge because of several factors such as weather, EV state, traffic conditions, and nonlinear relation between battery SOC and open circuit voltage (OCV). Generally, ampere-hour integration,[1,2] open-circuit voltage method,[1,3] neural network,[4,5] and Kalman filtering[6–8] are used for battery SOC estimation. Ampere-hour integration is the most commonly used method as it is theoretically the most precise method for SOC estimation. However, the estimation accuracy of this method highly relies on the initial SOC value and current measurement error, which make the ampere-hour integration method inapplicable. In real-time system, the open-circuit voltage method is only used to estimate initial SOC. As for Neural network, it is a huge burden for a microprocessor to estimate multiple SOC

a)Electronic mail: xz@home.swjtu.edu.cn

values using a large amount of experimental data. Kalman filtering is an intelligent algorithm for estimating the current of the time-varying state of a dynamic system. It might be a suitable approach applied in EV. However, it still has a disadvantage that the convergence of Kalman filtering highly relies on accurate battery models.

This paper presents an SOC estimation method for battery packs which reduces the effects of the initial SOC value and current measurement errors, e.g., measurement noise and drift. The SOC estimation algorithm is still robust even with the disturbance of voltage sensor missing with a relatively short duration. First, an improved Thevenin equivalent circuit model that can express battery characteristics more accurately is proposed. Second, open-circuit voltage method, ampere-hour integration, and Kalman filtering are combined as the SOC estimation algorithm. Finally, the proposed battery model and the SOC estimation algorithm are verified through both simulations and experiments. In fact, the long plateau in the voltage profile of batteries such as $LiFePO_4$ increases the difficulty in battery modelling. The modelling and SOC estimation methods proposed in this paper can be extensively applied onto recently developed lithium-ion batteries[9,10] for fast charge/discharge applications, whose voltage profile is sloped without a plateau.

II. BATTERY MODEL AND SOC ESTIMATION ALGORITHM

A. The improved Thevenin equivalent model

It is well-known that battery parameters are different when it is under charging or discharging conditions, as well as at different SOC.[11] In order to get the $LiFePO_4$ battery behaviors under charging and discharging conditions, respectively, the traditional Thevenin equivalent circuit model[12] of $LiFePO_4$ battery, as shown in Figure 1(a), is improved. Figure 1(b) presents the improved battery equivalent circuit, where U_{oc} is an ideal voltage source to represent the open circuit voltage of battery cell, I_o is the load current, U_o is the battery output voltage, I_p is the battery polarization current, C_p is the polarization capacitor, R_i and R_p are the battery internal resistor and polarization resistor, respectively, where subscripts c and d mean charging and discharging. With the help of these diodes in the equivalent circuit, different internal and polarization resistors will be adopted during battery charging and discharging. Furthermore, the range of SOC is divided into 10 segments, and corresponding values of R_i, R_p, and τ are identified for each segment.

For a single $LiFePO_4$ battery, the variable calculation equations are acquired by choosing SOC and I_p as system state variables, U_o as system output, I_o as system input. I_o is positive during discharging and negative during charging.

The discrete expression of SOC based on ampere-hour integration is as below (1):

$$SOC(k) = SOC(k-1) - \eta[I_o(k) + I_o(k-1)][T(k) - T(k-1)]/2C, \tag{1}$$

where C represents the battery static capacity, η is the coulombic efficiency which is different under charging and discharging conditions, k is the time index, and T is the sampling instance. The initial SOC value is calculated by open-circuit voltage method.[1,3]

The calculation of state variable I_p is as expression (2)

$$I_p(k) = \left[1 - \frac{1 - e^{-\Delta T/\tau}}{\Delta T/\tau}\right] I_o(k) + \left[\frac{1 - e^{-\Delta T/\tau}}{\Delta T/\tau} - e^{-\Delta T/\tau}\right] I_o(k-1) + e^{-\Delta T/\tau} \times I_p(k-1), \tag{2}$$

where τ is the time constant of polarization to represent the battery dynamic response, and $\Delta T = T(k) - T(k-1)$.

Expression (3) represents the battery output

$$U_o = U_{oc} - R_i I_o - R_p I_p, \tag{3}$$

where U_{oc} is the OCV of battery and its relationship with SOC is nonlinear. The value of R_i and R_p is different due to battery charging or discharging conditions. In this paper, linear interpolation is employed to obtain the segmented linearized expression of OCV related to SOC

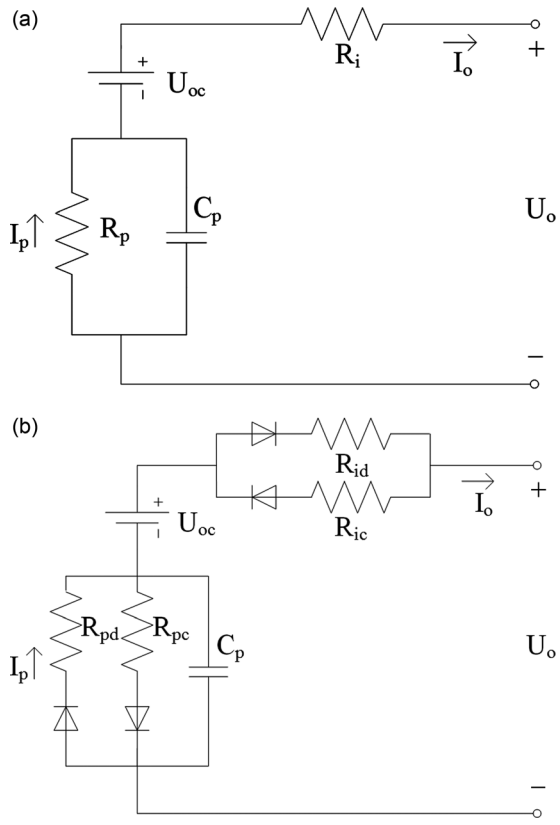

FIG. 1. Equivalent circuit models of $LiFePO_4$ battery (a) the traditional Thevenin equivalent circuit model. (b) The improved Thevenin equivalent circuit model.

$$U_{oc}(k) = OCV = \frac{OCV_{end} - OCV_{start}}{SOC_{end} - SOC_{start}}[SOC(k) - SOC_{start}] + OCV_{start} + C_c \ or \ C_d, \tag{4}$$

where subscripts "start" and "end" represent the start and the end of every segment, respectively, C_c and C_d are compensation values for the OCV when the battery is charging and discharging.

The system can be expressed in a discrete-time state-space form from expression (1) and (2), as below:

$$\begin{bmatrix} SOC(k) \\ I_p(k) \end{bmatrix} = \begin{bmatrix} 1 & 0 \\ 0 & e^{-\Delta T/\tau} \end{bmatrix} \begin{bmatrix} SOC(k-1) \\ I_p(k-1) \end{bmatrix} + \begin{bmatrix} \frac{\eta \Delta T}{2C} \\ 1 - \frac{1 - e^{-\Delta T/\tau}}{\Delta T/\tau} \end{bmatrix} I_o(k) + \begin{bmatrix} \frac{\eta \Delta T}{2C} \\ \frac{1 - e^{-\Delta T/\tau}}{\Delta T/\tau} - e^{-\Delta T/\tau} \end{bmatrix} I_o(k-1). \tag{5}$$

The system output function can be derived from expression (3) and (4)

$$U_o(k) = \begin{bmatrix} \frac{OCV_{end} - OCV_{start}}{SOC_{end} - SOC_{start}} & R_p \end{bmatrix} \begin{bmatrix} SOC(k) - SOC_{start} \\ I_p(k) \end{bmatrix} + OCV_{start} - I_o R_i + C_c \ or \ C_d. \tag{6}$$

B. Kalman filtering based SOC estimation

Kalman filtering[13] is a set of mathematical equations that provides an efficient computational recursive method to estimate the state of a dynamic system, even though the initial state is uncertain or the measurement is incomplete due to noise.

Assuming a discrete system in expression (7) and (8)

$$x_k = A_k x_{k-1} + B_k u_k + \omega_k, \tag{7}$$

$$z_k = H_k x_k + \upsilon_k, \tag{8}$$

where x_k is the state vector, u_k is the input vector, and z_k is the measurement vector. A_k is the state matrix, B_k is the input matrix, and H_k is the measurement matrix. The random variables ω_k and υ_k represent the process and measurement noises, respectively, which are assumed to be independent and with normal probability distributions.

At time step k, the prior estimation of system states and their estimated error covariance matrix are

$$\hat{x}_k^- = A_k \hat{x}_{k-1} + B_k u_{k-1}, \tag{9}$$

$$P_k^- = A P_{k-1} A^T + Q, \tag{10}$$

where Q is the process noise covariance matrix. Then, the Kalman gain or blending factor matrix K_k that minimizes the posterior error covariance can be updated accordingly

$$K_k = \frac{P_k^- H^T}{H P_k^- H^T + R}, \tag{11}$$

where R is the measurement noise covariance matrix.

Therefore, the posterior estimation of system states and their estimated error covariance matrix can be acquired

$$\hat{x}_k = \hat{x}_k^- + K_k(z_k - H\hat{x}_k^-), \tag{12}$$

$$P_k = (I - K_k H) P_k^-, \tag{13}$$

where I is identity matrix.

The system state matrix A based on the system state function derived from the proposed improved Thevenin equivalent circuit model can be written as below:

$$A = \begin{bmatrix} 1 & 0 \\ 0 & e^{-\Delta T/\tau} \end{bmatrix} \tag{14}$$

and the system measurement matrix H as

$$H = \begin{bmatrix} \dfrac{OCV_{end} - OCV_{start}}{SOC_{end} - SOC_{start}} & R_p \end{bmatrix}. \tag{15}$$

Substituting matrix A and H into the expressions (9)–(13), the equation for $LiFePO_4$ battery SOC estimation can be derived.

III. PARAMETERS IDENTIFICATION

In order to identify the parameters of the improved Thevenin equivalent circuit model in Figure 1(b), experiments are conducted on a 50 A h $LiFePO_4$ battery.

A. Battery static capacity and coulombic efficiency

Battery static capacity and coulombic efficiency are used for SOC calculation based on ampere-hour integration. In order to identify the static capacity, the battery is fully charged and discharged at C/3 rate constant current. The battery static capacity can be calculated by

integrating the charging and discharging currents. One hour rest for the testing battery is required between the charging and discharging processes. The average static capacity by multiple tests is 48.5 A h. The battery voltage curves under constant charging and discharging are shown in Figure 2.

After static capacity identification, the battery is fully charged and discharged at different current rates in order to find out the relationship between the coulombic efficiency and current.[14]

The coulombic efficiency as a function of the battery current is as follows:

$$\eta = \begin{cases} -0.0001I_o + 0.99 & (I_o > 0) \\ \dfrac{0.9896}{-0.00026I_o + 0.99} & (I_o < 0). \end{cases} \tag{16}$$

B. The OCV vs SOC curve

In order to find the relationship between OCV and SOC, the battery is fully charged and discharged at the C/25 rate.[6] This low rate is used to minimize the influence of the internal resistor on the battery output voltage. However, there still exists a gap between the charging and discharging terminal voltages, known as hysteresis as shown in Figure 3. In order to eliminate such hysteresis, the average battery terminal voltage is calculated based on the charging and discharging voltage obtained in this set of experiments. It can be assumed that the average voltage is approximately the same as OCV. In real applications, a compensation value is added or subtracted from the averaged OCV during charging or discharging accordingly.

C. Identification of R_i, R_p, and τ

The internal resistors, polarization resistors, and time constants of the improved Thevenin equivalent circuit model could be identified by the pulse charging and discharging tests, as shown in Figure 4. The data recorded in this set of experiments include current, voltage, time, and SOC, as shown in Figure 4.

Ten sets parameters of R_i, R_p, and τ are calculated by Linear Regression and Least Square methods from the experimental data mentioned above. Based on these parameters, taking one charging pulse as an example, the measured voltage and the battery output voltage calculated in Equation (6) are plotted in Figure 5. The error between the measured and estimated battery

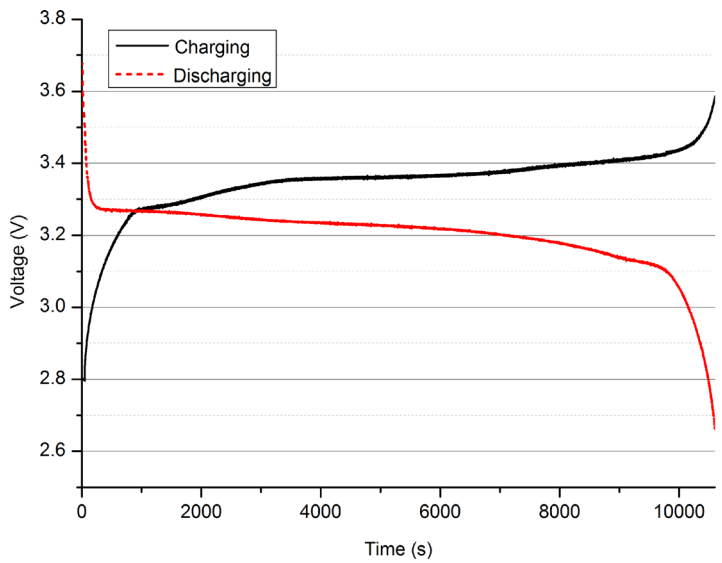

FIG. 2. Battery voltages under charging and discharging.

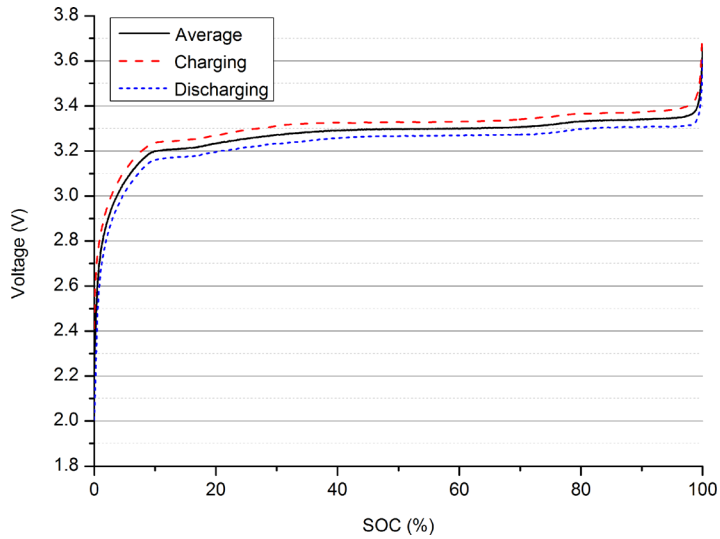

FIG. 3. OCV vs SOC.

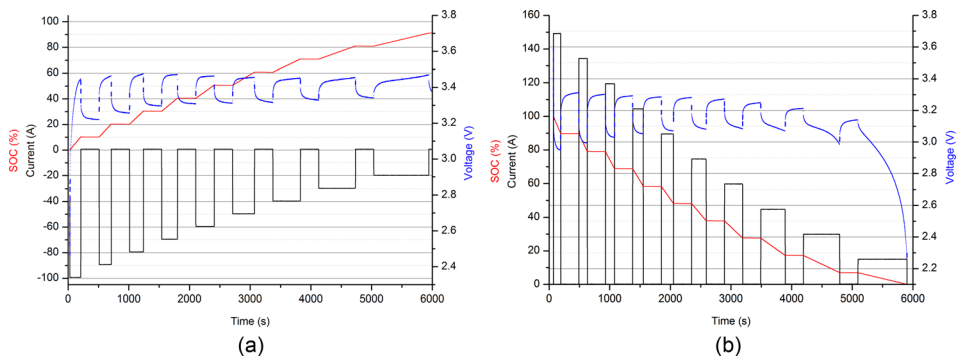

FIG. 4. Battery current, voltage, and SOC in pulse charging and discharging tests (a) charging and (b) discharging.

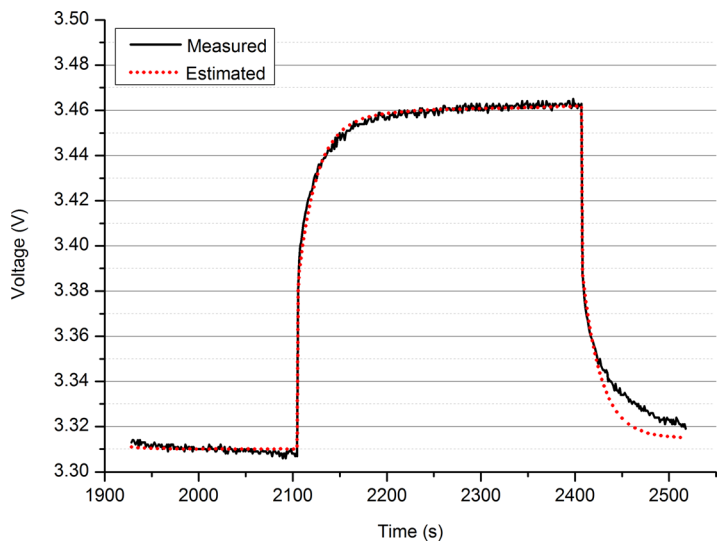

FIG. 5. Battery output voltage in one charging pulse.

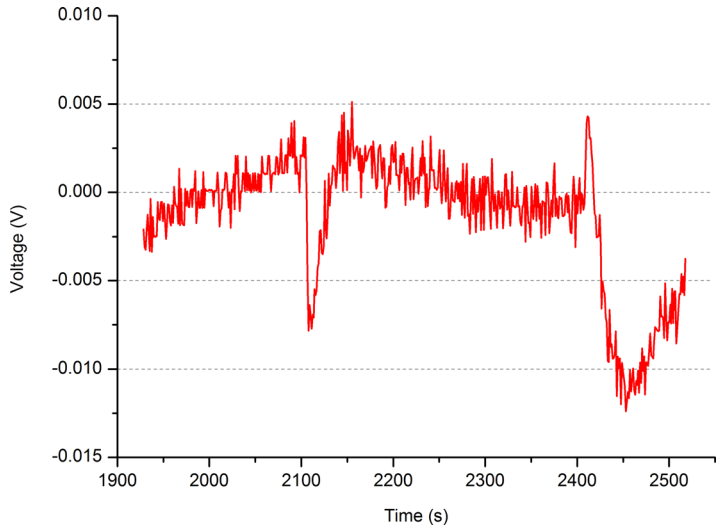

FIG. 6. Battery voltage estimation error.

output voltages is shown in Figure 6. It can be seen that the battery output voltage estimation error fluctuates within a range of 0.02 V (0.54% of battery max voltage).

IV. SIMULATION AND ANALYSIS

The parameters of the battery module in Simulink are set according to the manufacturer's datasheet of 50 A h $LiFePO_4$ battery as shown in Table I. The parameters of the traditional and the improved Thevenin equivalent circuit models are obtained by applying the same identification method to the battery module in Matlab/Simulink. Both models are established in Embedded MATLAB Function and Hybrid Pulse Power Characterization (HPPC) test[11] is adopted as load profile.

A. Verification of battery models

Since the voltage is the only output of the battery model, the estimation error of the output voltage represents the accuracy of the model. The estimated output voltages and the estimated errors are shown in Figures 7 and 8. A statistical analysis and comparison on the absolute values of the terminal voltage errors are conducted and the results are shown in Table II. The data of the last discharging segment (SOC between 10% and 0%) is excluded in analysis because battery is rarely discharged to empty in practical applications. Figure 8 shows that small estimation errors of the battery output voltage exist during large current step changes which is mainly determined by the identified resistances and the battery current. The estimation errors of the improved model are much smaller than that of the traditional model. The relatively larger error can only be found during a small period of time when there is a current step change.

TABLE I. Battery parameters in the manufacturer's datasheet.

Battery type	Nominal capacity (A h)	Max capacity (A h)	Nominal voltage (V)	Max voltage (V)	Min voltage (V)	Internal resistance (mΩ)
$LiFePO_4$	50	52.5	3.2	3.65	2.0	2.5
Cathode	Anode	Electrolyte	Width (mm)	Length (mm)	Height (mm)	Weight (kg)
$LiFePO_4$	Graphite	EC-DMC[a]	44	147	132.5	1.75

[a]Ethylene carbonate-dimethyl carbonate.

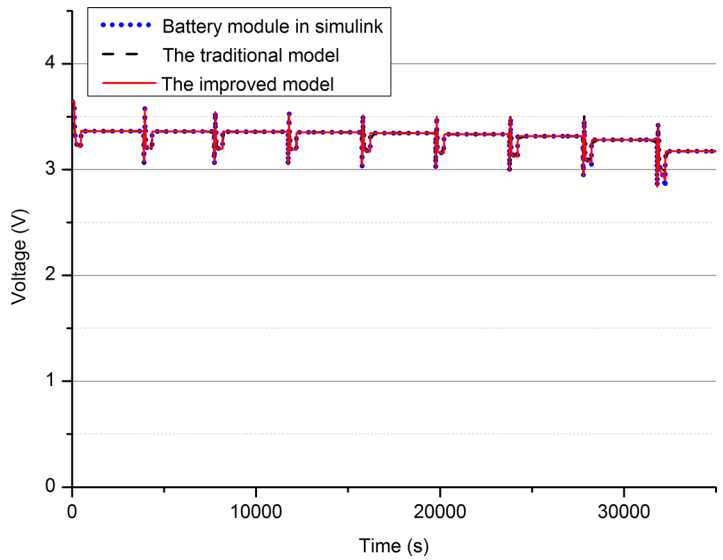

FIG. 7. Battery output voltages in the simulation.

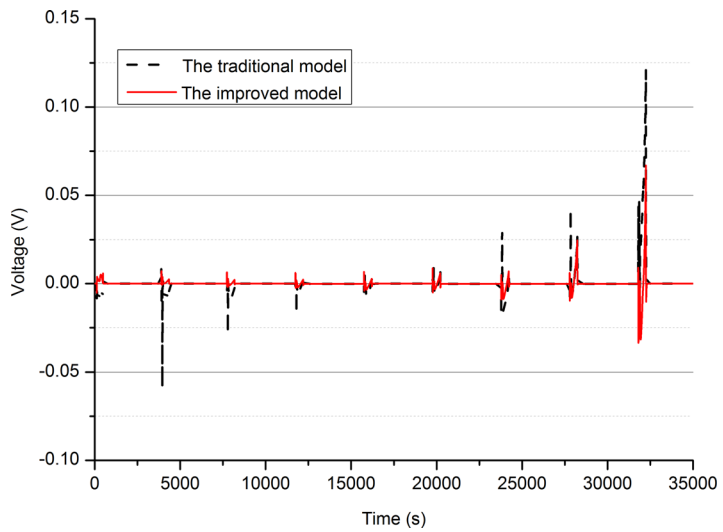

FIG. 8. Voltage estimation errors in the simulation.

From these curves and the comparison table, it can be seen that the voltage estimation error based on the improved model is within a range of 0.067 V, while that of the traditional model fluctuates within a range of 0.121 V. According to the simulation results, it is clearly proved that the improved model has higher accuracy and characterizes the dynamic response of the $LiFePO_4$ battery better. It also verifies the validity of the battery model and parameter identification method.

TABLE II. Statistical analysis list of the absolute values of battery terminal voltage in simulation.

Model	Max error (V)	Mean error (V)	Std. deviation (V)	Error rate (%)
The traditional model	0.121	0.0012	0.0066	0.181
The improved model	0.067	0.00055	0.003	0.082

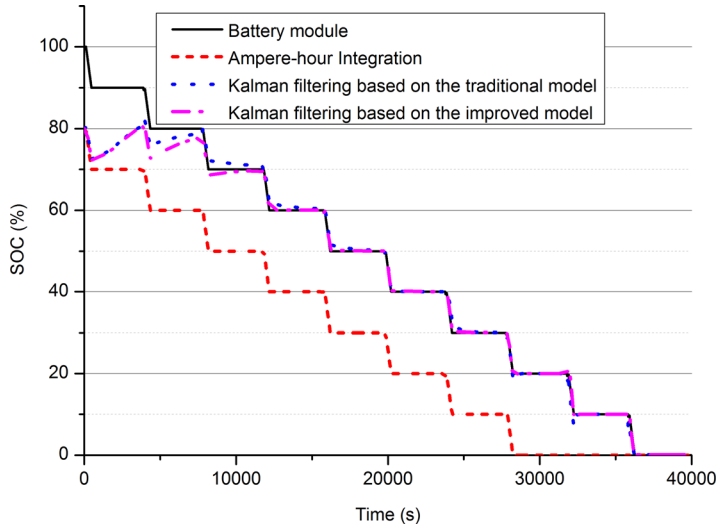

FIG. 9. Battery SOC curves in the simulation.

B. Verification of SOC estimation algorithm

The proposed SOC estimation algorithm was applied on both models. The initial SOC value is set to 80%, while the actual initial SOC value is 100%. The SOC estimation results of the two models with an initial error 20% are shown in Figure 9.

From the curves in Figure 9, it can be observed that there is always a 20% gap between the actual SOC and SOC estimated by ampere-hour integration. The estimated SOC based on Kalman Filtering reduces the error from 20% to 0% after certain cycles of iterations. In Figure 10, under the same circumstance, the SOC estimation based on the improved model converges to the actual value faster and more accurately than that of the traditional model. It obviously verifies the effectiveness of the proposed SOC estimation algorithm.

V. EXPERIMENTS AND ANALYSIS

The experimental platform consists of 1 kW electronic load KIKUSUI PLZ1004W, 1 kW DC power supply Chroma 6260-60 series, NI data acquisition module USB6009, and Hall effect current sensor HAIS 50-P.

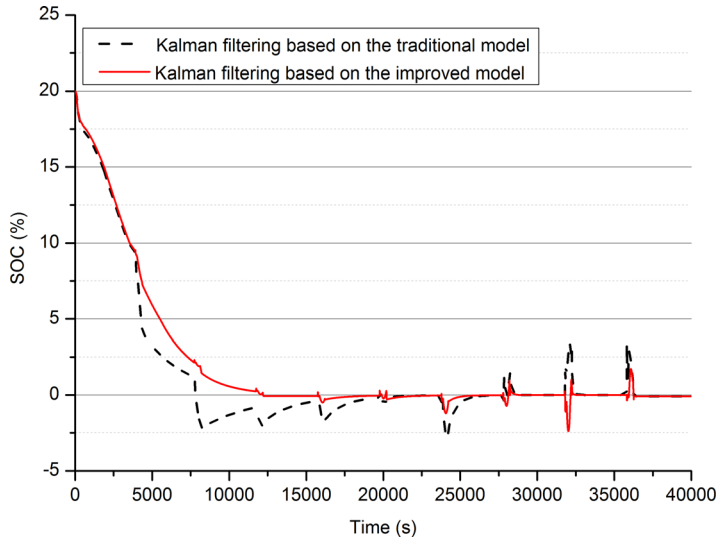

FIG. 10. SOC estimation errors in the simulation.

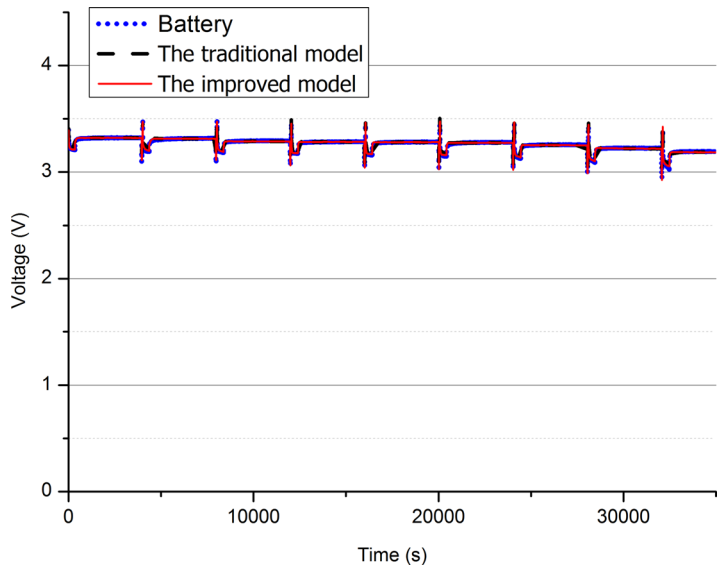

FIG. 11. Battery output voltages.

A. Verification of battery model

The experimental verification of the proposed battery model is presented in this subsection. The estimated battery output voltages and the estimation errors are shown in Figures 11 and 12, respectively. The data of the last discharging segment (SOC between 10% and 0%) are excluded. The statistical analysis of the terminal voltage estimation errors is presented in Table III. It can be seen that the improved model presents the battery characteristic very well, with the peak output voltage estimation error less than 0.0887 V. Since large estimation errors only occur during considerable load current step changes, the standard deviation of the estimation error can present the voltage estimation accuracy better. The standard deviation of the voltage estimation error obtained based on the improved battery model during the HPPC process is 0.00708 V (0.22% of the battery nominal voltage). The improved model can present the battery characteristics better than the traditional Thevenin equivalent circuit model does.

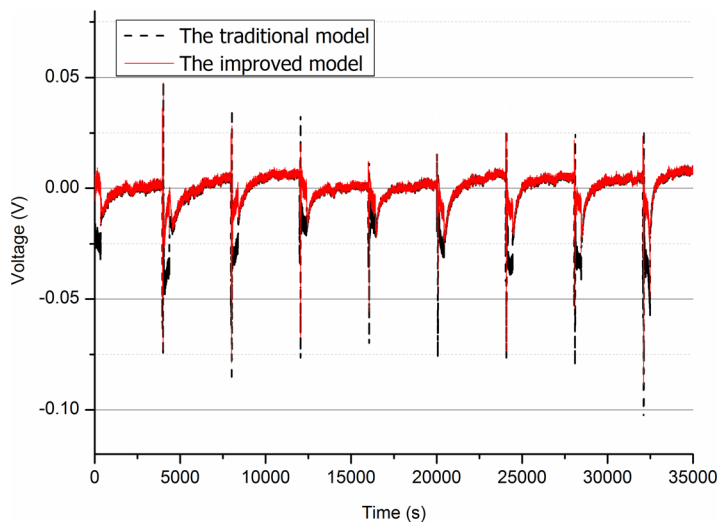

FIG. 12. Voltage estimation errors.

TABLE III. Statistical analysis list of the absolute values of battery terminal voltage in experiments.

Model	Max error (V)	Mean error (V)	Std. deviation (V)	Error rate (%)
The traditional model	0.1039	0.0083	0.01507	0.413
The improved model	0.0887	0.0014	0.00708	0.194

B. Verification of SOC estimation algorithm

In practical applications, current measurement errors are unavoidable. These measurement errors can be introduced by parameter drift of current measurement circuitry and environmental noise. The robustness of the proposed SOC estimation method with current measurement errors has been investigated experimentally. The SOC estimation results during discharging and charging obtained by the proposed algorithm and ampere-hour integration method, respectively, are presented in Figure 13.

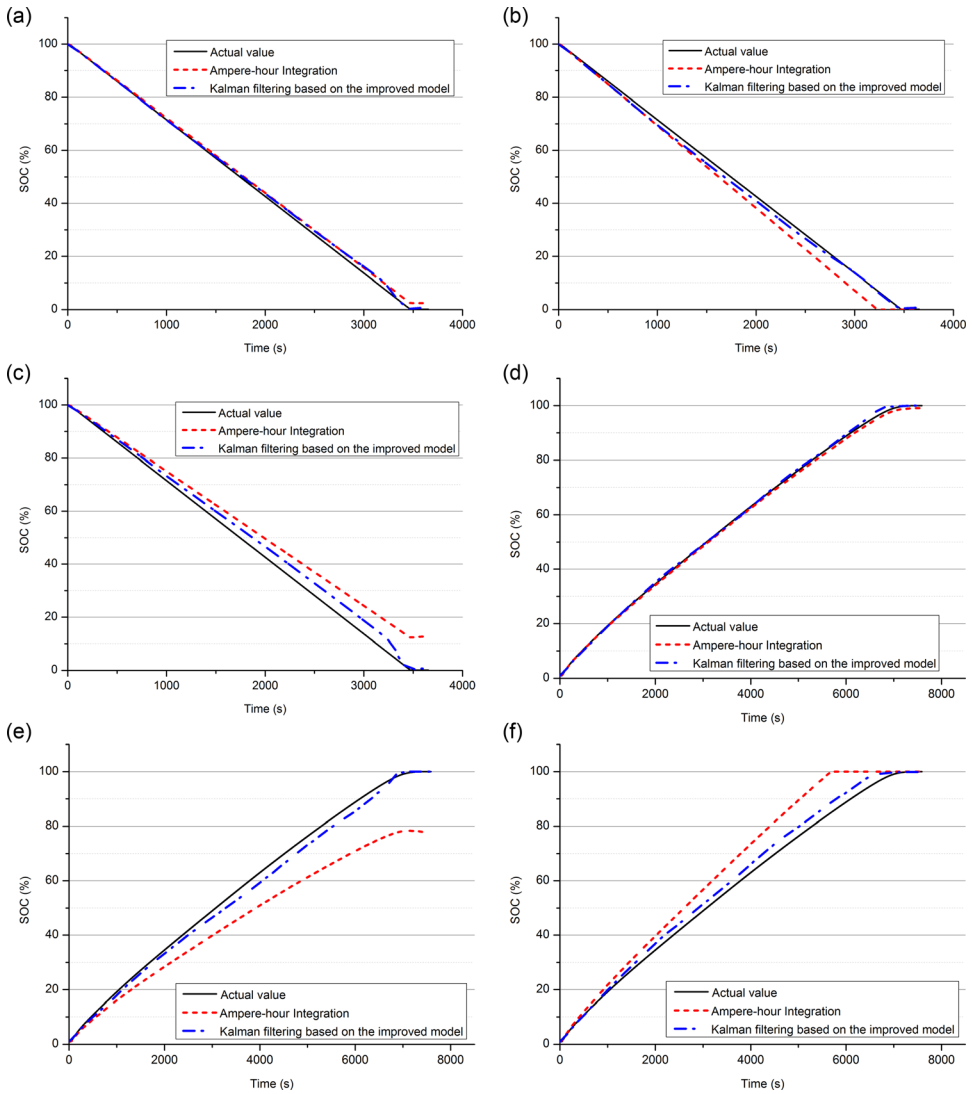

FIG. 13. SOC estimation with current measurement errors (a) Gaussian white noise is added into measured current (discharging); (b) the measured current is drifted by 5 A with Gaussian white noise (discharging); (c) the measured current is drifted by −5 A with Gaussian white noise (discharging); (d) Gaussian white noise is added into measured current (charging); (e) the measured current is drifted by 5 A with Gaussian white noise (charging); and (f) the measured current is drifted by −5 A with Gaussian white noise (charging).

In the first set of experiments, only the Gaussian white noise with zero mean has been added into the measured current. The standard deviation of the noise is set to be 5 to make the difference of the estimation results more distinguishable. Figures 13(a) and 13(d) show that the normally distributed noise with zero mean has little influence on the SOC estimation results.

In the next two sets of experiments, the measured currents have been shifted by ± 5 A, respectively, with Gaussian white noise whose standard deviation is one. It can be seen in Figures 13(b), 13(c), 13(e), and 13(f) that the current measurement drift might lead to significant SOC estimation error if the ampere-hour integration method is adopted. On the other hand, the proposed SOC estimation algorithm shows much more robust performance when there is a current measurement drift.

Another possible disturbance in real applications is that the output of the voltage sensor might be missing, which means that the measured voltage is constantly zero for a period of time. The performance of the proposed SOC estimation algorithm under such disturbance is evaluated as well. The estimation results have been presented in Figure 14.

In Figure 14(a), the output of the voltage sensor is set to 0 V at 600 s, 1200 s, and 1800 s, respectively, during the charge process, representing the voltage sensor missing disturbance. The duration of the disturbance is set to be 10 s. In Figure 14(c), the measured voltage is set to be 0 V at 2000 s, 4000 s, and 6000 s, respectively, with the same duration. The SOC estimation results illustrated in Figures 14(a) and 14(c) show that the proposed algorithm is robust under voltage sensor missing disturbance with relatively short duration.

In Figures 14(b) and 14(d), the outputs of the voltage sensor are not recovered after being set to 0 V at 1800 s (discharge) and 3600 s (charge), respectively. The SOC estimation results in Figures 14(b) and 14(d) drop dramatically to zero within 185 s, which will trigger the low SOC alarm and corresponding protections to prevent further damages to the system. Although the SOC estimation result obtained by the proposed estimation algorithm is incorrect in these two cases, it can be used to detect the fault of the voltage measurement circuitry and trigger the

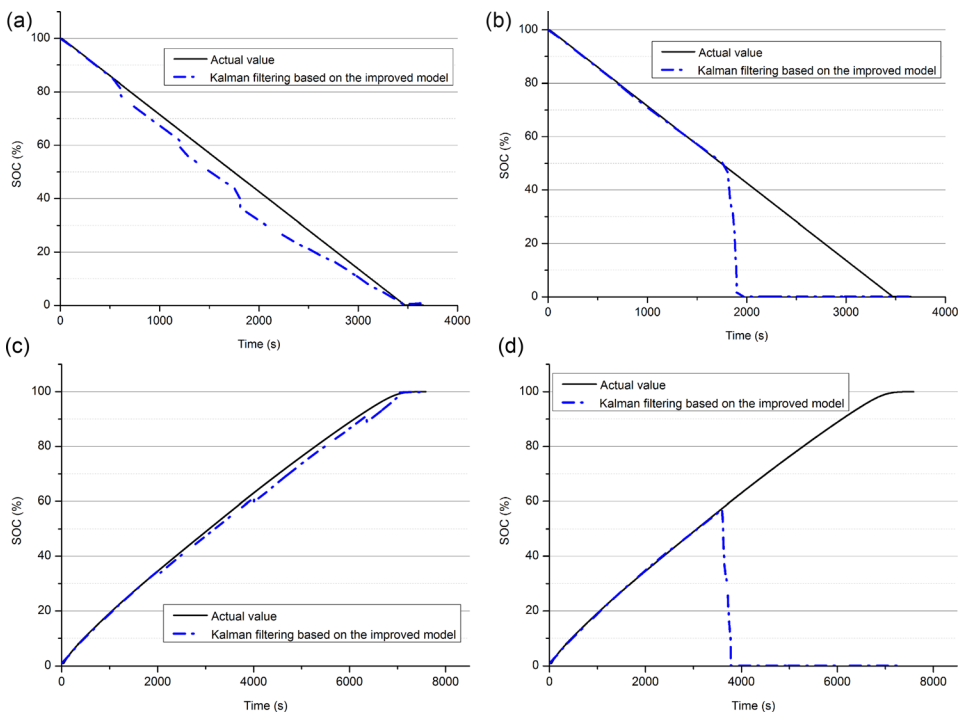

FIG. 14. SOC estimation with voltage sensor missing disturbance (a) 10-s voltage sensor missing disturbances (discharging); (b) unrecovered voltage sensor missing disturbance (discharging); (c) 10-s voltage sensor missing disturbances (charging); and (d) unrecovered voltage sensor missing disturbance (charging).

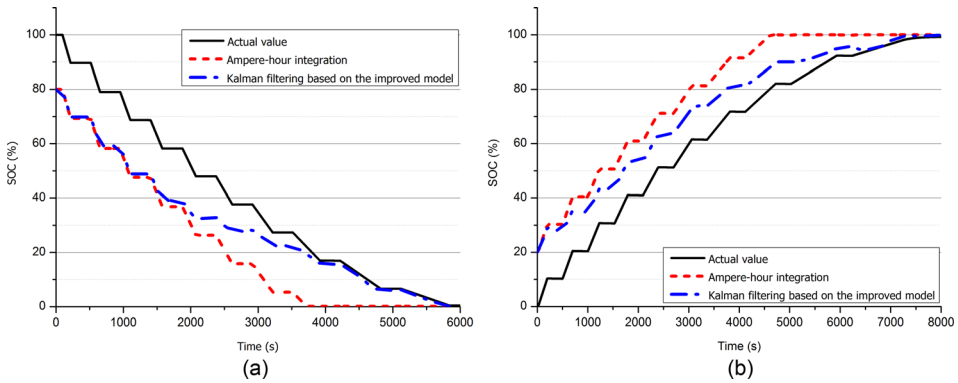

FIG. 15. SOC estimation of single battery (a) discharging and (b) charging.

protection, which will significantly increase the safety and reliability of the battery management system and the battery pack.

In this set of experiments, the battery was tested under the load profile shown in Figure 4. The initial SOC is intentionally set to be 20% differing from the actual SOC. It can be seen in Figure 15 that the SOC estimation based on the proposed method eventually converges to the actual SOC value. Meanwhile, the 20% gap always exists between the actual SOC and the SOC estimated by ampere-hour integration method. Such estimation error introduced by the incorrect SOC initial value would lead to a misjudgment of battery state and result in a tremendous waste of battery capacity or battery damage. It clearly shows that the proposed algorithm is effective in correcting the SOC estimation with initial error.

The same experimental process (referring to load profile in Figure 4) was conducted on two batteries connected in series and the results are presented in Figure 16. The initial SOCs of these two batteries are calculated by open-circuit voltage method. The experimental results apparently show that, under the same charging or discharging rate, the SOC estimations of these two batteries are different because the initial SOC values, battery parameters, and performances are different from each other. According to the results, the states and performances of the batteries connected in series can be distinguished by the proposed SOC estimation method. This feature can be used to indicate the SOC of individual battery and diagnose the battery performance degradation. With the help of the individual SOC indication, the active balancing techniques are able to be implemented in a battery management system. Furthermore, the batteries with degraded performance can be prevented from damages caused by over-charging and over-discharging with the accurate individual SOC estimation.

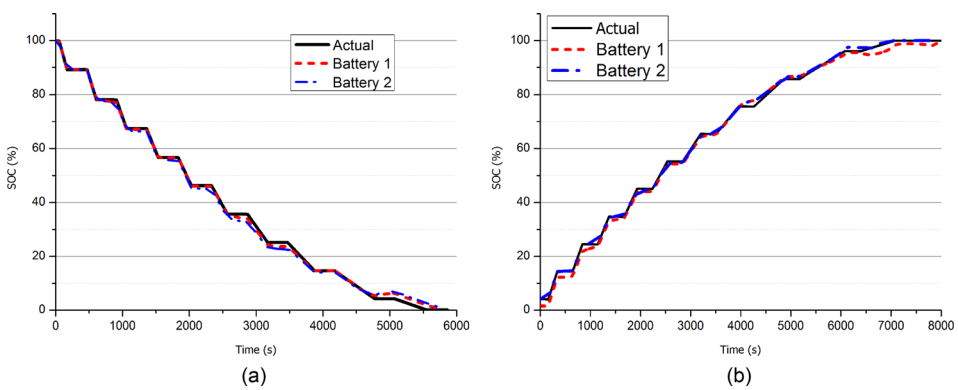

FIG. 16. SOC estimation of series batteries (a) discharging and (b) charging.

VI. CONCLUSION

The improved Thevenin equivalent circuit model is established based on the characteristics of the $LiFePO_4$ battery in this paper. The proposed SOC estimation algorithm is combined with the open-circuit voltage method, ampere-hour integration, and Kalman filtering based on the improved model. The conclusions obtained from simulation and experiments are as follows:

(1) The improved Thevenin equivalent circuit model with identified parameters accurately reflects the $LiFePO_4$ battery static and transient process under charging and discharging conditions, which is helpful for accurate SOC estimation.
(2) The effectiveness of the proposed SOC estimation algorithm, even with an incorrect initial SOC value, has been proved in simulation and experiments. The robustness of the SOC estimation algorithm with current measurement errors and voltage sensor missing disturbances has been comprehensively investigated, and the experimental results have proved the robustness of the algorithm.
(3) The difference in performance of the series connected batteries can be distinguished from SOC estimation by the proposed algorithm which provides a reference for battery management strategy.

ACKNOWLEDGMENTS

We gratefully acknowledge Professor Liu Zhixiang and Associate Professor Li Qi for the valuable consultations and discussions regarding the composition of the paper.

[1]C. Lin, J. Wang, and Q. Chen, "Methods for state of charge estimation of EV batteries and their application," Battery Bimon. **34**(5), 376–378 (2004).
[2]K. S. Nga, C.-S. Mooa, Y.-P. Chenb, and Y.-C. Hsiehc, "Enhanced coulomb counting method for estimating state-of-charge and state-of-health of lithium-ion batteries," Appl. Energy **86**(9), 1506–1511 (2009).
[3]J. H. Aylor, A. Thieme, and B. W. Johnso, "A battery state of charge indicator for electric wheelchairs," IEEE Trans. Ind. Electron. **39**(5), 398–409 (1992).
[4]Z. Qi, F. Wu, S. Chen, Q. Yu, and G. Wang, "Research on forecast the state of charge of battery based on artificial neural network," Chin. J. Power Sources **29**(5), 325–328 (2005).
[5]P. Shi, C. Bu, and Y. Zhao, "The ANN models for SOC/BRC estimation of Li-ion battery," *IEEE in International Conference on Information Acquisition* (2005), pp. 560–564.
[6]G. L. Plett, "Extended Kalman filtering for battery management systems of LiPB-based HEV battery packs—Part 1. Background," J. Power Sources **134**(2), 252–261 (2004).
[7]G. L. Plett, "Extended Kalman filtering for battery management systems of LiPB-based HEV battery packs—Part 2. Modeling and identification," J. Power Sources **134**(2), 262–276 (2004).
[8]Z. He, M. Gao, and J. Xu, "EKF-Ah based state of charge online estimation for lithium-ion power battery," IEEE Int. Conf. Comput. Secur. **1**, 142–145 (2009).
[9]V. Augustyn, J. Come, M. A. Lowe, J. W. Kim, P.-L. Taberna, S. H. Tolbert, H. D. Abruña, P. Simon, and B. Dunn, "High-rate electrochemical energy storage through Li+ intercalation pseudocapacitance," Nat. Mater. **12**, 518–522 (2013).
[10]K. Zhang, B. K. Michael, B. Li, J. K. Sung, X. Du, X. Hao, R. J. Jacob, S. Zhang, W. G. George, V. Anton, M. B. Bart, and X. Pan, "Water-free Titania-Bronze thin films with superfast lithium-ion transport," Adv. Mater. **26**, 7365–7370 (2014).
[11]United States Idaho National Engineering & Environmental Laboratory, "Freedom car battery test manual for power-assist hybrid electric vehicles," Report No. DOE/ID-11069, 2003.
[12]C. Lin, B. Qiu, and Q. Chen, "Comparison of current input equivalent circuit model of electric vehicle batteries," Chin. J. Mech. Eng. **41**(12), 76–81 (2005).
[13]R. E. Kalman, "A new approach to linear filtering and prediction problems," J. Basic Eng. **82**, 35–45 (1960).
[14]W. Huang, X. Han, Q. Chen, and C. Lin, "A study on SOC estimation algorithm and battery management system for electric vehicle," Automot. Eng. **29**(3), 198–202 (2007).